JOURNAL OF CATALYSIS 26, 352–358 (1972)

Structural Evolution of Molybdenum Sulfide Catalysts

P. RATNASAMY AND A. J. LÉONARD

Laboratoire de Physico-Chimie Minérale, Institut des Sciences de la Terre, de Croylaan, 42, 3030 Héverlée, Belgium

Received September 30, 1971

Molybdenum sulfide samples of varying surface areas were prepared by the reduction in H_2 of MoS_3 at 250, 350, 450, 550 and 800°C. From their X-ray diffractograms, changes occurring in their crystal structure are deduced. These deductions are supported by observed changes in the surface area. Together, they make possible some speculations concerning the dependence of the catalytic activity of molybdenum sulfide on the temperature of pretreatment.

INTRODUCTION

Molybdenum sulfide catalysts are widely used in hydrogenation and hydrodesulfurization reactions. Usually supported on Al_2O_3 or SiO_2–Al_2O_3, they are used either alone or along with cobalt oxide (commercially known as "cobalt–molybdate") for vapor phase catalytic hydrodesulfurization of thiophene. Even in cases where the oxide is the starting material, it is converted partially to the sulfides during the hydrodesulfurization reaction. The crystal structure of MoS_2, which occurs in nature as the mineral molybdenite, has been investigated by Dickinson and Pauling (*1*). Its crystal lattice is built up of layers and has a hexagonal symmetry. MoS_3 prepared, for example, by the procedure of Moldavski *et al.* (*2*) is amorphous to X-rays. Its structure is not known with certainty. Prolonged heating at 1100°C in vacuum is necessary to convert MoS_3 to well-crystallized hexagonal MoS_2 (*3*). The molybdenum sulfide used in many catalytic reaction studies, however, is obtained by reduction of MoS_3 in H_2 at 400–500°C. No systematic study of the changes in structure accompanying the above treatment in H_2 has yet been reported. X-Ray diffraction techniques have been utilized in the present study to follow the structural evolution of molybdenum sulfide. The corresponding changes in the surface area are also reported.

EXPERIMENTAL METHODS

Materials

Sample A was MoS_3 prepared according to the method of Moldavski *et al.* (*2*). H_2S was passed through an aqueous solution of ammonium paramolybdate to saturation. The solution was then warmed. The brown precipitate obtained on neutralizing with HCl was filtered and dried at 110°C.

Samples B, C, D, E and F were prepared from sample A by reduction for 10 hr in a quartz tube in a stream of dry H_2 at 250, 350, 450, 550 and 800°C, respectively. For each heating, a new sample of the trisulfide was used. Sample G was MoS_2 (BDH).

Apparatus

The surface areas were determined by a dynamic procedure (*4*). Nitrogen was used as the adsorbate at the temperature of liquid nitrogen. Copper $K\alpha$ radiation from a Philips X-ray diffractometer was used in the X-ray studies along with nickel filters.

RESULTS

1. Surface Area

The surface areas for samples A–G were 29.6, 23.6, 28.7, 34.6, 80.2, 30.5 and 19.5 m^2/g, respectively. Thus the surface area decreases initially and thereafter increases regularly to reach a maximum after treatment around 550°C. Further increase in temperature leads to a drastic reduction in surface area.

2. X-Ray Diffraction Analysis

The powder diffractograms of samples A–G are shown in Fig. 1. The *d* spacings and the corresponding *hkl* indices of the planes were calculated from the spectra of Fig. 1 and are given in Table 1, together with the relative intensities and peak shapes. The dimensions of the hexagonal unit cell are given in Table 2. In addition to the hexagonal form, a rhombohedral form of MoS_2 has also been reported (*3*). Some of the lines observed for sample F could be indexed only when the presence of the rhombohedral form is taken into account. These are also indicated in Tables 1 and 2. Sample G was found to be pure hexagonal MoS_2. In agreement with Wildervanck and Jellinek (*3*), MoS_3 (sample A) is found to be amorphous (Fig. 1, curve A).

In all the curves, the 002 peak is the most intense. This indicates strong orientation around the *c* axis. This is due to the fact that no extra precaution was taken to avoid orientation of the crystallites before their X-ray pattern was taken. It may be mentioned here that molybdenum sulfide catalysts are usually used in pellet form. Strong orientation of the crystallites will thus undoubtedly be present in those catalysts also.

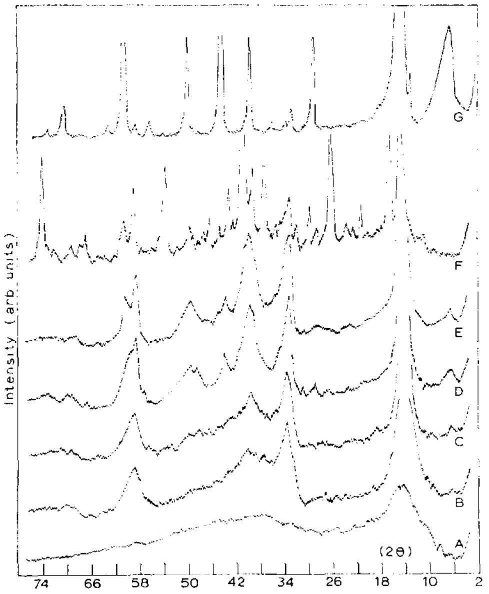

FIG. 1. X-Ray diffractograms of samples A–G.

After heating at 250°C, the 002 line of hexagonal MoS_2 is well developed. It becomes narrower as the temperature of reduction is raised. The 101 and 110 lines can also be discerned at 250°C even though they are much broader. In addition, the 101 line is asymmetric in shape with a comparatively sharp front and a long tail towards the larger angles. This asymmetry of the 101 line becomes more and more accentuated and is very clearly seen in curves D and E (Fig. 1). The significance of this observation is discussed below.

At 350°C, the 101 line becomes sharper and the 103 line becomes more resolved from the 101 line, though it is still very broad. The 001 line begins to appear as a minor broad peak at $2\theta = 6.5°$.

At 450°C, this 001 line as well as the 103 line are more prominent. The 101 line, while being more intense, is also more asymmetric. A new line at $2\theta = 44.0°$, characteristic of the (006) planes also appears at 450°C. An interesting feature of curve D is the split in the 105 line. It is probably the nonequivalence of the (105) and (015) planes in the structure that is at the origin of this phenomenon. The broad shoulder in the higher angle side of the 110 line evolves into the 112 line at 550°C which, though broad, is still fairly symmetric. An additional point to note at 550°C is the merger of the doublet of the 105 and 015 lines (curve D) into a single, though broad band. The material obtained after heating in H_2 at 800°C for 24 hr is much more crystalline as may be seen from the many narrow lines in the X-ray pattern (curve F). Both hexagonal and rhombohedral forms of MoS_2, are apparently present. In Table 1, the *hkl* indices for the rhombohedral form are given using the hexagonal axes system. They are indicated in parentheses in column 11. The unit cell parameters for the rhombohedral form are given in Table 2. These compare well with those of Wildervanck and Jellinek (*3*) ($a =$

TABLE 1

X-RAY DIFFRACTION RESULTS FOR SAMPLES A–G[a]

Samples												
	B		C		D		E		F		G	
A	*d* (Å)	*hkl*	*d* (Å)	*hkl*	*d* (Å)	*hkl*	*d* (Å)	*hkl*	*d* (Å)	*hkl*[b]	*d* (Å)	*hkl*
Amorphous	6.108$_5$ (100)	002 (Vb.s)	13.598$_0$ (4)	001 (Vb.as)	13.598$_8$ (6)	001 (Vb.as)	13.598$_0$ (6)	001 (b.s)	6.108$_5$ (100)	002 (ns)	13.192$_0$ (40)	001 (bas)
	2.674$_9$ (44)	101 (Vb.as)	6.108$_5$ (100)	002 (bs)	6.108$_5$ (100)	002 (bs)	6.108$_5$ (100)	002 (b.s)	5.372$_3$ (85)	(004) (ns)	6.558$_7$ (20)	(ns)
	1.572$_8$ (25)	110 (Vb.as)	2.674$_9$ (39)	101 (b.as)	2.690$_5$ (50)	101 (b.as)	2.690$_5$ (52)	101 (b.as)	4.114$_0$ (21)	003 (ns)	6.108$_5$ (100)	002 (nas)
			2.281$_3$ (26)	103 (Vb.as)	2.270$_3$ (44)	103 (b.s)	2.253$_9$ (52)	103 (b.s)	3.401$_2$ (81)	(005) (ns)	3.068$_5$ (57)	004 (ns)
			1.565$_5$ (22)	008, 110 (Vb.s)	2.057$_9$ (19)	006 (b.s)	2.057$_9$ (19)	006 (Vb.s)	3.110$_4$ (11)	004 (bas)	2.730$_8$ (10)	100 (nas)
					1.869$_7$ (13)	015 (b.as)	1.837$_8$ (17)	105 (Vb.s)	2.998$_0$ (25)	(006) (ns)	2.674$_9$ (5)	101 (bas)
					1.577$_7$ (35)	110 (b.as)	1.575$_2$ (37)	110, 008 (n, s)	2.805$_3$ (14)	100 (ns)	2.494$_7$ (5)	102 (bas)
					1.837$_8$ (16)	105 (b.as)	1.530$_2$ (25)	112 (b.s)	2.698$_4$ (31)	101 (bas)	2.275$_8$ (41)	103 (nas)
									2.592$_3$ (17)	(007) (bas)	2.031$_6$ (90)	104 (ns)
									2.528$_6$ (15)	102 (bas)	1.824$_1$ (40)	105 (ns)
									2.398$_2$ (54)	005 (ns)	1.698$_0$ (2)	007 (bs)

2.292_4 (54)	103 (nas)	1.636_7 (5)	106 (bs)
2.211_6 (95)	(105) (ns)	1.577_7 (5)	008, 110 (bas)
2.127_0 (15)	(008) (ns)	1.532_5 (85)	112 (ns)
2.089_5 (38)	(009) (nas)	1.475_4 (3)	113 (bs)
2.027_3 (12.3)	104 (bas)	1.339_0 (12)	202 (bs)
1.952_9 (17)	(106) (bs)	1.296_0 (2)	203 (bs)
1.914_1 (7)	(107) (bs)		
1.834_4 (12)	105 (bs)		
1.703_9 (57)	007 (ns)		
1.565_5 (43)	008, (110) (ns)		
1.530_2 (17)	112 (bs)		
1.400_4 (7)	114 (bs)		
1.384_0 (5)	009 (bas)		
1.361 (5)	201 (bas)		
1.280_9 (69)	(205) (nas)		

---

[a] Vb.as = very broad asymmetric; bs = broad symmetric; Vbs = very broad symmetric; bas = broad asymmetric; ns = narrow symmetric; nas = narrow asymmetric.

[b] The *hkl* index values for the rhombohedral MoS_2 are indicated in parentheses for sample F.

TABLE 2
Unit Cell Dimensions of Samples B–G

Sample	a (Å)	c (Å)	c/a	V [cell vol (Å³)]
B	3.17	12.22	3.85	106.38
C	3.17	12.22	3.85	106.38
D	3.17	12.22	3.85	106.38
E	3.17	12.22	3.85	106.38
F hex.	3.24	12.22	3.77	110.01
rhom.	3.17	18.41	5.81	160.12
G	3.15	12.27	3.89	105.61

3.163 Å, $c = 18.37$ Å; $c/a = 5.808$; and $V = 159.3$ Å³). For the hexagonal MoS_2, the corresponding values of Wildervanck and Jellinek are $a = 3.1602$ Å, $c = 12.294$ Å; $c/a = 3.8902$ and $V = 106.34$ Å³. These values also compare well with those of sample G in Table 2. A major difference between the patterns of commercial MoS_2 (sample G) and those of samples A–F is the presence of strong 001 and 004 lines in the former and their negligible intensity in the latter. In fact, the 004 line is absent in all the synthetic samples (A–F) and the 001 line is present only to a minor extent in samples B to E.

Discussion

In the hydrodesulfurization of thiophene, molybdenum sulfide catalysts attain their maximum activity around a reaction temperature of 400–550°C. At higher temperatures, the activity falls steeply (*6*). In the hydrodesulfurization of thiophene over MoS_2, Kolboe and Amberg (*5*) have noted a decrease in activity per unit area when the catalyst was reduced in H_2/He mixtures at 650°C. They suggested that this could be due to "thermal destruction of unstable surface states in the MoS_2 crystallite, of surface impurities or of microcracks accessible only to N_2 or combinations of these factors."

Let us now consider what changes in the structure might be responsible for the reduction in catalytic activity and surface area. Figure 2 shows the hexagonal structure (*1*) of MoS_2. It is built up of layers, each layer containing either molybdenum or sulfur atoms. Each molybdenum atom is surrounded by six sulfur atoms at the vertices of a trigonal prism. In the mineral molybdenite, which belongs to the hexagonal form (as well as our sample G) subsequent layers are in antiparallel orientation (*3*). Each layer is related to its neighboring layers by a translation along the c axis followed by a rotation of 180° around the c axis. In the rhombohedral form (which is present in our sample F), how-

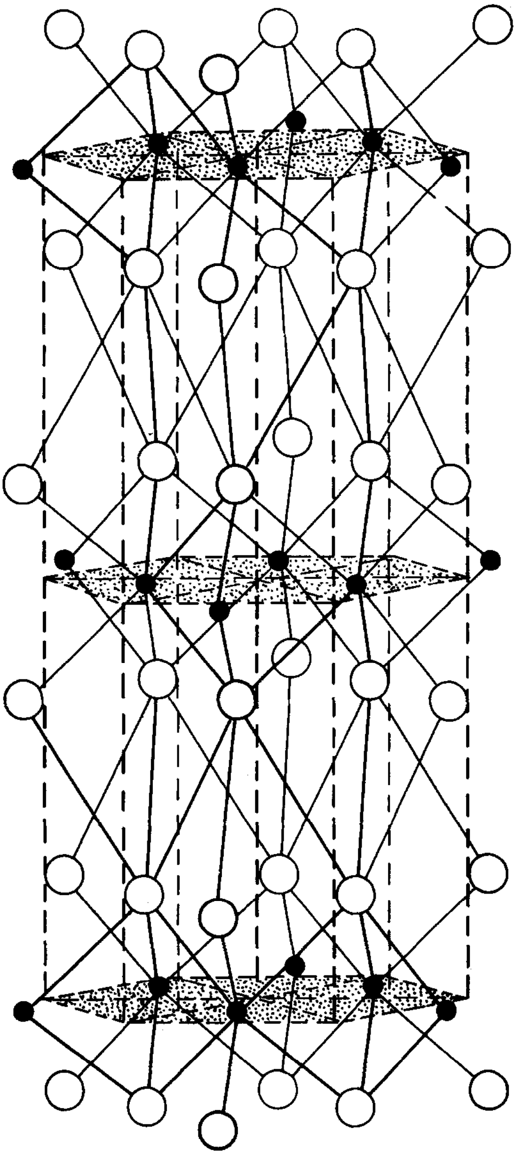

Fig. 2. The structure of hexagonal MoS_2: (●) molybdenum atoms; (○) sulfur [Ref. (*1*)].

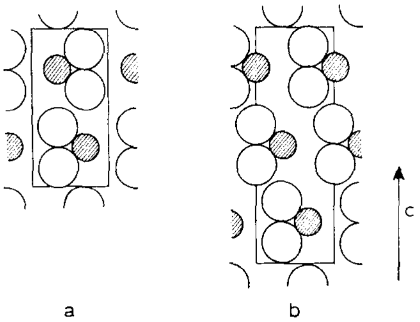

FIG. 3. Sections through the (110) plane of (a) hexagonal MoS_2 and (b) rhombohedral MoS_2 [Ref. (*3*)].

ever, adjacent layers are related to each other by a translation only (*3*). This is clearly shown in Fig. 3 where sections through the (110) plane in both hexagonal (a) and rhombohedral (b) forms of MoS_2 are shown (*3*).

During the formation of MoS_2 from ammonium paramolybdate, the liberation of gases like H_2O, H_2S and NH_3 leads to a porous body with a high surface area (sample E). Small crystallites of MoS_2, if formed, are so randomly oriented that no lines are observed in the spectrum (curve A, Fig. 1).

At 350°C, the crystallites grow in size. The appearance of the 103 line points to the greater order of the atomic arrangement in the corresponding planes. But the material is still far from crystalline as may be seen from the broad bands.

A special feature of curves D and E is the strong asymmetry of the 101 line. Wilson (*7*) has analyzed the occurrence of such a phenomenon. In our case, it means that in the direction perpendicular to the (101) planes, the type of ordering is not the same throughout each single crystal but "changes step" occasionally.

Thus, the probability of cells separated by a distance, say t (in a direction perpendicular to the (101) plane) being the same decreases with increasing t. It may be noted that the (101) plane in MoS_2, unlike the (001) planes, contain both molybdenum and sulfur. Defects in this plane would certainly play a role in the catalytic activity of these planes.

At 450°C, as well as at 550°C, both parallel and antiparallel stacking of adjacent layers occurs almost at random. The differentiation between the (105) and (015) planes (at 450°C) implies an additional loss of symmetry in the structure.

Wilson (*8*) has discussed in detail the asymmetric line profiles of *hkl* reflections from layer materials. A semiquantitative treatment of the broadening and displacement of the lines leads to the equation:

$$\Delta\theta = 0.16\,\lambda/P\cos\theta,$$

where θ is the Bragg angle, $\Delta\theta$ is the displacement of the peak maximum from the calculated value, λ is the wavelength of the X-radiation and P is the square root of the area of a layer. Applying this equation to the asymmetric line profile of the 110 reflection for sample D ($\Delta\theta = 0.1$, $\lambda = 1.5418$), a value of P equal to 8.0 Å^2 is calculated. For sample G ($a = 3.15$ Å), the area per layer is 8.59 Å^2.

The layers in sample D are thus far from ideal. The smaller layer area, reflecting highly disordered layers, is also the cause of the larger surface area for this sample.

The greater defective nature of the crystal lattice in sample D is also probably the cause of the greater catalytic activity shown by Kolboe and Amberg (*5*) in catalysts taken to 450°C. At lower temperatures, the activity is less. This is due to the smaller surface area. As more and more sulfur is removed by reduction in H_2 at increasing temperatures, the surface area of the material increases. This leads to greater catalytic activity. At higher temperatures, however, transformation to the more ordered rhombohedral form occurs (curve F). The concentration of structure defects is obviously reduced drastically. The destruction of these surface defects may explain the decrease in catalytic activity per unit area observed by Kolboe and Amberg (*5*).

The concentration of the new rhombohedral phase also increases with increasing temperature. This new phase probably has lower catalytic activity. These two factors combine to suppress the catalytic activity of samples reduced in H_2 above 550°C.

ACKNOWLEDGMENTS

The authors thank Professor J. J. Fripiat for encouragement and support. The technical assistance of Messers. J. C. Meeus and J. Breysem is gratefully acknowledged. The work was financially supported by IRSIA.

REFERENCES

1. DICKINSON, R. G., AND PAULING, L., *J. Amer. Chem. Soc.* **45**, 1466 (1923).
2. MOLDAVSKI, B. L., *J. Gen. Chem. USSR* **3**, 603 (1933).
3. WILDERVANCK, J. C., AND JELLINEK, F., *Z. Anorg. Allg. Chem.* 328 (1964).
4. CAHEN, R. M., MARÉCHAL, J. E. M., DELLA FAILLE, M. P., AND FRIPIAT, J. J., *Anal. Chem.* **37**, 133 (1965).
5. KOLBOE, S., AND AMBERG, C. H., *Can. J. Chem.* **44**(22), 2623 (1966).
6. MANN, R. S., *Indian J. Technol.* **3**, 53 (1965).
7. WILSON, A. J. C., *Proc. Roy. Soc. Ser. A* **181**, 360 (1943).
8. WILSON, A. J. C., "X-ray optics," p. 91. Methuen, London, 1962.